# CO$_2$/H$_2$ separation by amino-acid ionic liquids with polyethylene glycol as co-solvent

Jun Li [a,b], Zhongde Dai [a], Muhammad Usman [a], Zhiwen Qi [b,*], Liyuan Deng [a,*]

[a] Department of Chemical Engineering, Norwegian University of Science and Technology, Sem Sælandsvei 4, 7491 Trondheim, Norway
[b] State Key Laboratory of Chemical Engineering, School of Chemical Engineering, East China University of Science and Technology, 130 Meilong Road, Shanghai 200237, China

### ABSTRACT

In this work polyethylene glycol 400 (PEG400) was introduced as a co-solvent to intensify CO$_2$ separation and reduce the viscosity of amino-acid ionic liquids (AAILs) while maintain their unique properties, i.e. undetectable vapor pressure, high thermal stability and excellent CO$_2$ solubility. The thermal gravimetric analysis indicated that AAILs, PEG400 and their blend solvents were stable at above 523 K and showed negligible weight loss at 373 K for 300 min. The viscosity of the mixed solvents decreased to be about half of that of pure AAILs at 298 K. The CO$_2$ solubility in the mixed solution was measured over a range of pressures from 100 to 1700 kPa and of temperatures from 333.15 to 413.15 K at 40 K intervals. The ideal CO$_2$/H$_2$ selectivity reached 110 at 333.15 K and 100 kPa. PEG400 as a co-solvent may have created a better gas-liquid interface, which promotes the mass transfer and intensifies the CO$_2$ sorption in AAILs. A CO$_2$ absorption mechanism in AAILs-PEG400 was proposed accordingly to explain the intensification effect with evidence from the FTIR results.

© 2015 Elsevier Ltd. All rights reserved.

## 1. Introduction

The increasingly serious climate situation caused by large CO$_2$ emissions from fossil fuel-derived energy production has become a critical societal challenge and has caused serious public concern in recent years. The basic knowledge and innovative solutions for CO$_2$ capture techniques are widely studied. Meanwhile, significant progress has been achieved from three main CO$_2$ capture pathways, namely post-combustion, pre-combustion and oxy-fuel. Compared to the other two approaches, pre-combustion can be more economical and less energy intensive, as CO$_2$ in syngas is more concentrated and at a high CO$_2$ partial pressure, which increases the driving force for separation and largely reduces the energy consumption for compression. The size and cost of the capture facilities can be reduced as well. In addition, in pre-combustion process CO$_2$ is recovered before the fuel (H$_2$) is burned. It is beneficial for the downstream utilizations of H$_2$ and has a potential for reductions in further compression costs, if the purified H$_2$ is kept at high pressures. However, the separation of CO$_2$/H$_2$ and the relatively high operating temperature brings many challenges in developing practical separation techniques in pre-combustion CO$_2$ capture.

Well known as "green" solvents, ionic liquids can meet most of the requirements for pre-combustion CO$_2$ capture. Recently amino-acid ionic liquids (AAILs) have been reported to be a kind of promising CO$_2$ absorbents due to their excellent properties, such as high CO$_2$ sorption capacity, high thermal stability and negligible vapor pressure. Moreover, the relatively simple synthesis method by the neutralization reaction of a cation hydroxide solution and amino acid makes the production of AAILs inexpensive and environmentally friendly (Fukumoto et al., 2005; Gardas et al., 2010; Ohno and Fukumoto, 2007; Zhang et al., 2006; Zhang et al., 2012; Dai et al., 2016). However, the high viscosity impedes their further application in industry. For example, task-specific ionic liquids (TSILs) with an alkaline group or amino acid anions usually suffer from high viscosity from 300 mPa s to above 1000 mPa s at 298 K, and their viscosity further increases after absorbing CO$_2$ (Bates et al., 2002; Kagimoto et al., 2006). The relatively high cost is also a major drawback.

To address these problems researchers have started to focus on mixed solvents, such as the mixtures of task-specific ionic liquids (TSILs), water and amines (Baj et al., 2012; Jing et al., 2012; Zhang et al., 2010). These solvent blends show lower viscosity, competitive CO$_2$ sorption capacity and relatively faster absorption rates and lower cost. However, they are not suitable for operating at high

temperatures, as the presence of water and amines in the solvents counterweighs the advantages of the high thermal stability and low vapor pressure of TSILs. In recent years, the blends of TSILs and non-aqueous co-solvents with very low vapor pressure have also been investigated (Hasib-ur-Rahman et al., 2012; Li et al., 2012b; Shannon and Bara, 2011; Yang et al., 2011). The use of non-aqueous co-solvents takes the advantage of the low vapor pressure of TSILs, thereby being able to be used at higher temperatures than aqueous solvents. Moreover, they are more energy efficient as no extra heat will be consumed for the vaporization of co-solvent during the regeneration process (Chakma, 1997; Shannon and Bara, 2011). In addition, the solvent corrosion of steel will be reduced substantially under a non-aqueous environment (Hasib et al., 2012).

The use of membrane absorption is another approach to reduce the cost. In a membrane absorption process, a gas–liquid membrane contactor is the device that offers an effective gas–liquid mass transfer interface without dispersion of one phase to another. In combination with the advantages of both absorption processes and membrane separation, the membrane contactor is considered as a very efficient technique for $CO_2$ separation. It requires much smaller footprints and solvent holding for the same productivity, and has fewer moving parts, 30 times higher gas-liquid interface and lower energy consumption compared with conventional absorption processes (Hägg and Deng, 2015; Simons et al., 2009). Deng et al. have recently developed a new concept of $CO_2$ membrane absorption process using ionic liquid and a combined pressure swing–mild temperature swing absorption–desorption loop for pre-combustion $CO_2$ capture, which can be significantly more efficient and less energy intensive as compared to conventional absorption processes (Deng et al., 2014). Suitable absorbent with unique properties such as low vapor pressure and being thermally stable with a high $CO_2$ sorption capacity is the key to perform this combined pressure swing–mild temperature swing process. Except for its high $CO_2$ sorption capacity and $CO_2/H_2$ selectivity, a low viscosity in operating conditions is also critical, especially when a hollow fiber membrane contactor is used. Since solvents for this application must have both high thermal stability and low vapor pressure, the use of conventional amine-based aqueous solvents are therefore not practical for this application. It is therefore one of the biggest challenges to develop solvents with above mentioned properties in order to employ the membrane absorption process in pre-combustion $CO_2$ capture.

In this study, polyethylene glycols (PEGs) were introduced as a non-aqueous co-solvent to intensify the ability of AAILs to capture $CO_2$ in membrane absorption processes at relatively high operating temperatures. PEGs have the molecular structural formula $H(OCH_2CH_2)_nOH$, where $n$ is the number of ethylene oxide. PEGs have properties compatible with ILs, such as very low vapor pressure, non-toxicity, low cost and chemical and thermal stability (Aschenbrenner and Styring, 2010; Aschenbrenner et al., 2009; Li et al., 2012a). In addition, the physical properties of PEGs can be tuned by varying their molecular weights. PEGs have been widely used in the pharmaceutical, cosmetics, and food industries and recently as co-solvents for TSILs (Chen et al., 2007). Li et al. found (2-hydroxyethyl)-trimethyl-ammonium (S)-2-pyrrolidine-carboxylic acid salt using polyethylene glycol 200 (PEG200) as a co-solvent can enhance the rates of absorption and desorption of $CO_2$ from 298 to 353 K at ambient pressure (Li et al., 2008). However, for $CO_2$ capture, in pre-combustion conditions, absorbents with good performance at high temperatures (333–373 K or even higher) and at a wide range of pressures is required.

The aim of this work is to seek an available and market-inexpensive solvent with high thermal stability, low vapor pressure, high $CO_2$ sorption capacity and selectivity for the application of gas–liquid membrane contactors in pre-combustion process. Based on the screening of a broad range of different types of ionic liquids for the desired properties, three typical tetrabutylphosphonium ($[P_{4444}]^+$) based AAILs with glycine (Gly), alanine (Ala), and proline (Pro) as anions were chosen and investigated in this study. PEGs with molecular weight of 200, 300 and 400 were selected as potential co-solvents due to their relatively low viscosity and vapor pressure. The thermal stability of PEGs, AAILs and their mixtures were first investigated. Their density and viscosity were determined in temperatures ranging from 293.15 to 353.15 K and 298.15 to 393.15 K, respectively. These basic physical properties are important in the selection of suitable TSIL co-solvent for the target separation process. For example, the reduced viscosity contributes significantly to the intensification effect introduced to the separation system. The $CO_2$ absorption performance (including solubility, absorption mechanism and absorption rate) in the mixed solvents (30 wt% AAILs in PEG400) with a pressure range of 100–1700 kPa and a temperature range from 333.15 to 413.15 K at 40 K intervals were investigated. In order to evaluate the ideal $CO_2/H_2$ selectivity, the solubility of $H_2$ was also investigated at 333.15 K with a pressure range of 100–1000 kPa. Results show that AAILs-PEG400 solvents are suitable liquid absorbents for this designed membrane contactor process. These types of solvents are also suitable for $CO_2$ absorption in conventional absorbers, such as packed columns or tray columns, and for $CO_2$ separation from other sources such as biogas, natural gas and flue gas, with the benefits of being energy saving, low corrosion rate and environmentally friendly.

## 2. Materials and methods

### 2.1. Material

Polyethylene glycol 200 (PEG200, with an average molecular weight of 200), polyethylene glycol 300 (PEG300, with an average molecular weight of 300), polyethylene glycol 400 (PEG400, with an average molecular weight of 400), tetrabutylphosphonium hydroxide $[P_{4444}][OH]$ (40% by mass aqueous solution), glycine (Gly, 99%), alanine (Ala, 98%) and proline (Pro, 99%) were obtained from Sigma Aldrich. Hydrogen ($H_2$) and carbon dioxide ($CO_2$) with purity of 99.999% were supplied by Praxair. All materials were used as received without further treatment.

### 2.2. Synthesis of amino-acid ionic liquids

The $[P_{4444}]^+$ based AAILs were prepared according to previously reported methods (Fukumoto et al., 2005; Gardas et al., 2010; Kagimoto et al., 2006). The $[P_{4444}][OH]$ aqueous solution was added drop-wise to a slightly excess equimolar amino acid aqueous solution. The mixture was stirred at room temperature for 12 h, then water was evaporated at 318 K. A mixed solvent (9:1, v/v) of acetonitrile and methanol was added to this reaction mixture and stirred rigorously. The mixture was then filtered to remove any excess amino acid. Filtrate was evaporated to remove solvents. The product was dried in a vacuum for 48 h at 343 K to reduce water content and volatile compounds to undetectable values prior to their use. The purity of each AAIL was checked using $^1$H NMR spectra, which were recorded on a Bruker Avance DPX 400 MHz NMR spectrometer using dimethyl sulfoxide as the solvent (see Supporting Information, Figures SI1–SI3). The structures of the cation and anions of AAILs studied are shown in Fig. 1. The water contents of these ILs were determined by a Karl Fisher titration and found to be less than 0.2 wt%.

### 2.3. Apparatus and procedures

The thermal stability of PEGs, AAILs and their mixtures were investigated using Perkin Elmer (Pyris 1) instrument according to
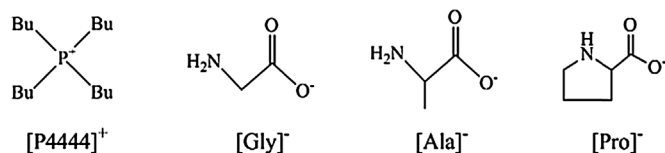
Fig. 1. The structures of the cations and anions of AAILs.

the thermal gravimetrical analysis (TGA) method. A known amount of sample (12–16 mg) in $N_2$ (60 mL/min) atmosphere was initiated at 298 K followed by a temperature increase to 800 K at a heating rate of 10.0 K/min. The density and viscosity of all solvents were determined using Anton Paar DMA 4500M apparatus and the rheometer (Physica MCR 100), respectively.

The vapor–liquid equilibrium (or solubility) apparatus and methods of analysis were similar to our previous work (Li et al., 2012a, 2014). About 10 g of AAIL and PEG mixture was weighed using an electronic balance (Sartorius, ±0.0001 g) and put into the absorption vessel. The system was controlled at the specific temperature ($T$) in an oil bath with an accuracy of 0.1 K. The chamber was evacuated using a vacuum pump to reach a pressure of <2 kPa. A pressure transducer (Series 33X, Keller) with an accuracy of 0.2 kPa was used to record the pressure ($P$) variation at an interval of 1 s. Equilibrium was considered to be reached after more than 2 h absorption and the pressure being stabilized for 1 h. The volumes of the gas storage tank ($Vg$) and the gas absorption vessel ($Va$) are 80.7 ± 0.1 mL and 33.9 ± 0.1 mL, respectively. The volume of the liquid in the vessel was calculated by the weight and density data. The pressure drop method and the Soave–Redlich–Kwong (SRK) equation of state from $PVT$ data were employed to calculate the $CO_2$ solubility in the solvent.

## 3. Results and discussion

### 3.1. Thermal stability

A good thermal stability of a solvent is critical with respect to solvent regeneration at elevated temperatures. Taking the problem of corrosion and degradation into consideration, conventional aqueous alkanolamine solutions are usually regenerated at about 393 K (Lee et al., 2013). However, the much higher absorption and regeneration temperature in pre-combustion process requires absorbents to have a much better thermal stability than alkanolamine solutions (Notz et al., 2011).

Fig. 2 illustrates the thermal gravimetric results of pure PEGs and AAILs. The thermal stability of pure solvents is in the order of:

**Table 1**
The onset temperature and viscosity of pure PEGs and AAILs.

| | $M$/g mol$^{-1}$ | $T_{onset}$/K, this work | $T_{onset}$/K, ref. | $\eta$/mPa s |
|---|---|---|---|---|
| PEG200 | ~200 | 461 | 475[a] | 38.7 (at 303 K)[d] |
| PEG300 | ~300 | 500 | 545[a] | 70.1 (at 298 K) |
| PEG400 | ~400 | 566 | – | 69.6 (at 303 K)[d] |
| [P$_{4444}$][Gly] | 333.5 | 535 | 566[b] | 415 (at 298 K)[b] |
| [P$_{4444}$][Ala] | 347.5 | 530 | 559[b] | 344 (at 298 K)[b] |
| [P$_{4444}$][Pro] | 373.6 | 536 | 587[b], 572[c] | 851 (at 298 K)[b] |

[a] Aschenbrenner and Styring (2010).
[b] Kagimoto et al. (2006).
[c] Gardas et al. (2010).
[d] Trivedi and Pandey (2011).

PEG400 > AAILs > PEG300 > PEG200. In this study, the onset temperature ($T_{onset}$, defined as the intersection of the baseline weight and the tangent line derived from the dropping curve) was employed to indicate the temperature where weight loss begins on the TGA, as listed in Table 1. The weight loss can be attributed to total evaporation or decomposition of the sample. The $T_{onset}$ of PEG200, PEG300 and PEG400 are around 461 K, 500 K and 566 K, respectively. Hence, PEGs with higher molecular weights showed better thermal stability, but also higher viscosity, as listed in Table 1. Aiming at different practical $CO_2$ capture temperatures, available PEGs can be selected after balancing their thermal-stability and viscosity. Three selected AAILs show similar $T_d$ of about 530 K, which also indicates a good thermal stability at high temperatures. It should be noted that the $T_{onset}$ of pure solvents are lower than the reference data. This behavior can be attributed to the different amounts of samples, rate of carrier gas and heating rate, which have a great influence on $T_{onset}$. For example, Aschenbrenner reported that the higher amounts of samples (20–40 mg vs 12–16 mg) and lower rate of carrier gas (50 mL/min vs 60 mL/min) lead to a relatively higher $T_{onset}$ of PEG200 and PEG300 (Aschenbrenner and Styring, 2010). Although there are some differences in $T_{onset}$, it suggests that both PEG400 and AAILs have good thermal stability above 530 K. As a result, PEG400 was selected as co-solvent in this study.

To further study the thermal stability of mixtures, their long-term thermal performances were analyzed at 373 K and 413 K for 300 min in $N_2$ (60 mL/min), as illustrated in Fig. 3. In this study, all AAILs-PEG400 mixtures consisted of 30 wt% AAILs and 70 wt% PEG400. At 373 K, the weight loss percentages for [P$_{4444}$][Gly]-PEG400, [P$_{4444}$][Ala]-PEG400, [P$_{4444}$][Pro]-PEG400 are 0.29%, 0.24% and 0.24%, respectively. In our previous work, the weight loss percentages for alkanolamine-PEG200 at 353 K were recorded as varying between 8% and 26% in $N_2$ (20 mL/min) (Li et al., 2014). It
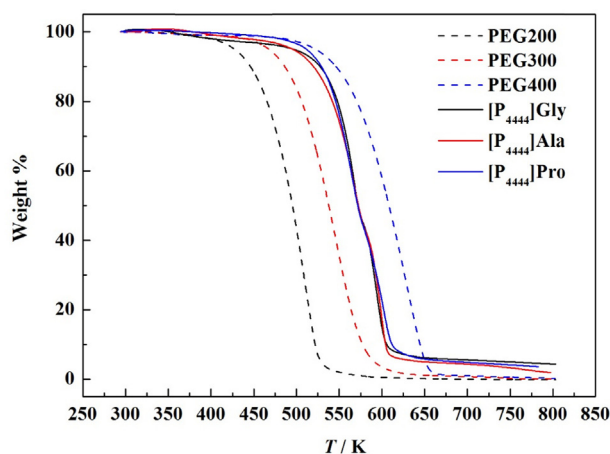


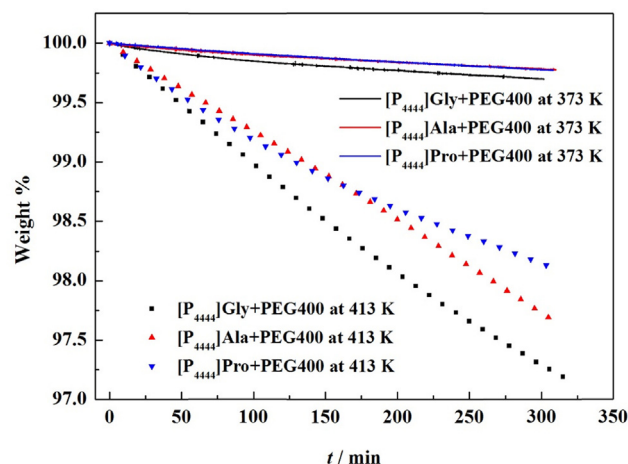Fig. 2. TGA curves of pure PEGs and AAILs.



Fig. 3. TGA curves of 30 wt% AAILs + 70 wt% PEG400 at constant temperatures.

can be concluded that AAILs-PEG400 solutions have a much better thermal stability than the alkanolamine-PEG solutions. When the temperature increased to 413 K, the weight loss percentages for [P$_{4444}$][Gly]-PEG400, [P$_{4444}$][Ala]-PEG400, [P$_{4444}$][Pro]-PEG400 increased to 2.72%, 2.28% and 1.92%, respectively, which are still much more stable than the reported amine-contained solvent at lower temperatures. The small amounts of weight loss may be resulted from the evaporation of solvents under the N$_2$ purging conditions at high temperatures. As a result, the mixed solvents of AAILs and PEG400 showed good thermal stability and very low volatility even when temperature reached 413 K.

### 3.2. Density

The physical properties of solvents are essential for designing absorption processes and providing operational instructions. This is particularly important for membrane absorption processes, as density and viscosity are critical properties when analyzing feasibility and the optimization of the membrane contactor. Moreover, density was also an important parameter to calculate the gas phase volume in absorption vessel according to pressure drop method.

Density measurements of mixed solvents AAILs-PEG400 were carried out at temperatures ranging from 293.15 to 353.15 K at 0.1 MPa. The experimental density data obtained are listed in Table SI1. The density of mixed solvents decreased in the following order:   [P$_{4444}$][Pro]-PEG400 > [P$_{4444}$][Gly]-PEG400 > [P$_{4444}$][Ala]-PEG400, which is consistent with the density order of pure AAILs reported in references (Gardas et al., 2010; Zhang et al., 2006). Fig. 4 illustrates the variation of the density with temperature for the mixed solvents. As can be seen, the density of all solvents decreases as temperature increases. The density can be correlated for temperature dependence as Eq. (1) (Gardas et al., 2010) with the parameters a and b given in Table 2 together with the absolute average deviation (AAD).

$$\rho/(\text{g cm}^{-3}) = a/(\text{g cm}^{-3}) + b \cdot T/\text{K} \qquad (1)$$

The AAD is defined as:

$$\text{AAD} \ (\%) = \frac{\sum_{i=1}^{N_p} |(\rho_{cal} - \rho_{exp})/\rho_{exp}|_i}{N_p} \times 100 \qquad (2)$$

where cal and exp denote the calculated and experimental data, respectively, and $N_p$ represents the number of experimental data points. The density correlations for AAILs-PEG400 solutions fit the density results with AAD below 0.01%. The apparent linear relation observed in Fig. 4 between density and temperature has already been reported by several authors in pure AAILs or mixtures of alkanolmines and PEG400 (Davis et al., 1993; Goodrich et al., 2010). Hence, the density of AAILs-PEG400 at 373 K and 413 K can be estimated according to the equation, and then be used to calculate the solubility at these temperatures based on SRK equation from the PVT data.

### 3.3. Viscosity

High viscosity is a major drawback in the application of AAILs in CO$_2$ absorption processes. Viscosity significantly influences the mass transfer and hence process efficiency. Therefore, low viscosity is one of the most important requirements for the solvent developed in this study.

The viscosities of mixed solvents AAILs-PEG400 and pure PEG400 were determined at temperatures ranging from 298.15 K to 393.15 K at 0.1 MPa, as listed in Table SI2 and plotted in Fig. 5. At 298.15 K, the viscosity of mixed AAILs-PEG400 is about half the viscosity of pure AAILs (as shown in Table 1) due to the relatively low viscosity of PEG400. When the temperature increases to 333.15 K, the viscosity shows a dramatically decrease. For example, the viscosity of [P$_{4444}$][Ala]-PEG400 decreases from 216.64 to 44.52 mPa s as temperature increased from 293.15 to 333.15 K. The viscosity further decreases to about 10 mPa s as the temperature increases to 393 K. The viscosity of mixed solutions is no longer a problem for membrane absorption in the operating temperature range of the designed process (333–393 K).

An exponential viscosity-temperature correlation based on the VFT equation is proposed (Gardas et al., 2010):

$$\ln \eta = A + \frac{B}{(T - T_0)} \qquad (3)$$

where $\eta$ is viscosity in mPa s, $T$ is temperature in K, and $A$, $B$, and $T_0$ are correlation parameters. The ratio of parameters $B$ and $T_0$ ($B/T_0$) is known as the Angell strength parameter. All correlation parameters are listed in Table 3.
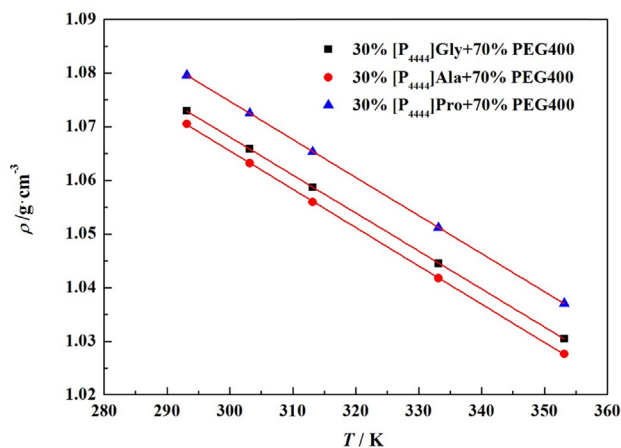


**Fig. 4.** Experimental density ($\rho$) of mixed solvents (30 wt% AAIL + 70 wt% PEG400) studied as a function of temperature at atmospheric pressure.

**Table 2**
Correlation parameters for density and temperature of mixed solvents AAILs-PEG400.

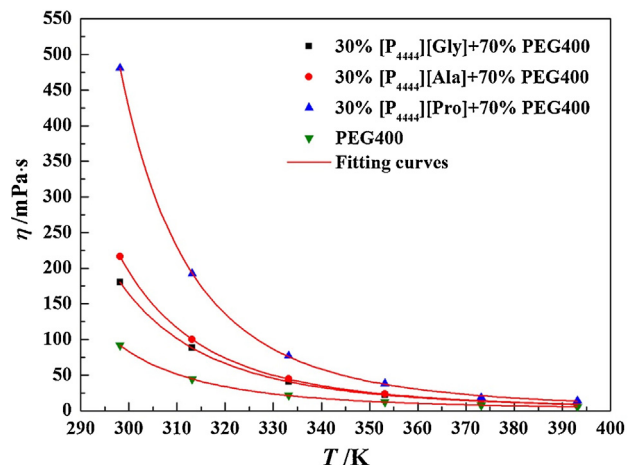|  | a/g cm$^{-3}$ | 10$^4$ b/K | AAD % |
|---|---|---|---|
| 30% [P$_{4444}$]Gly + 70% PEG400 | 1.28037 | −7.0769 | 0.004 |
| 30% [P$_{4444}$]Ala + 70% PEG400 | 1.27962 | −7.13793 | 0.009 |
| 30% [P$_{4444}$]Pro + 70% PEG400 | 1.28754 | −7.09405 | 0.004 |



**Fig. 5.** Experimental viscosity ($\eta$) of mixed solvents (30 wt% AAIL + 70 wt% PEG400) studied as a function of temperature at atmospheric pressure.

**Table 3**
Correlation parameters for viscosity and temperature of mixed solvents AAILs-PEG400.

|  | $A$ | $B$/K | $T_0$/K | $R^2$ |
|---|---|---|---|---|
| 30% [P$_{4444}$]Gly + 70% PEG400 | −2.397 | 1093.79 | 154.09 | 0.99999 |
| 30% [P$_{4444}$]Ala + 70% PEG400 | −2.178 | 996.81 | 166.23 | 1 |
| 30% [P$_{4444}$]Pro + 70% PEG400 | −1.720 | 905.70 | 183.40 | 0.9999 |
| PEG400 | −1.700 | 710.16 | 184.01 | 0.99992 |

### 3.4. CO$_2$ sorption in AAILs-PEG400 mixed solvents

Although the solubility of many pure TSILs has been widely reported, most of the data are available only at a temperature lower than 373 K and at ambient pressure. In this work, the equilibrium solubility was obtained for CO$_2$ in mixtures of PEG400 with [P$_{4444}$][Gly], [P$_{4444}$][Ala] and [P$_{4444}$][Pro] at (333.15, 373.15 and 413.15) K within a range of CO$_2$ partial pressure of 100–1700 kPa. The concentration of AAILs was 30 wt% with an uncertainty of 0.1 wt%. In this study, both CO$_2$ capacity ($\alpha$, mol CO$_2$/kg total solution) and CO$_2$ loading ($\beta$, mol CO$_2$/mol AAIL) were used to present CO$_2$ solubility in mixed solvents of AAILs-PEG400 at different temperatures and pressures, as listed in Tables SI3–SI5.

Fig. 6 illustrates the solubility of CO$_2$ in the mixed solvents based on CO$_2$ capacity $\alpha$. As can be seen, at 333.15 K and 100 kPa of CO$_2$ partial pressure, every kg of AAIL-PEG400 can absorb around 0.68 mol of CO$_2$. To reach the same CO$_2$ capacity for ionic liquid [bmim][BF$_4$], the pressure must be much higher and at a lower temperature (i.e. 1270 kPa at 313 K (Aki et al., 2004)). This indicates that AAIL-PEG400 has a much better CO$_2$ sorption capacity than conventional ionic liquids with physisorption, which is resulted from the combination of chemisorption and physisorption in the AAIL-PEG400 mixture. When CO$_2$ partial pressure is low, the chemical sorption of CO$_2$ in AAILs dominates the absorption process, which leads to a high CO$_2$ capacity even at high temperature. However, the reactive sites in AAILs are being saturated with increasing pressure, and eventually the physisorption of AAIL and PEG400 becomes dominating. This can be confirmed by the VLE curves, which show a linear tendency when pressure exceeds 200 kPa. As a result, the AAIL-PEG400 solution can be regenerated by a combined pressure and temperature swing method. For example, if the [P$_{4444}$][Gly]-PEG400 blend absorbs CO$_2$ at 333.15 K and 1700 kPa (CO$_2$ capacity 1.57 mol CO$_2$/kg solution), it can be regenerated by reducing the pressure to 100 kPa and increasing temperature to 413.15 K (CO$_2$ capacity 0.11 mol CO$_2$/kg solution); as a result, the cyclic CO$_2$ capacity reaches 1.46 mol CO$_2$/kg solution.
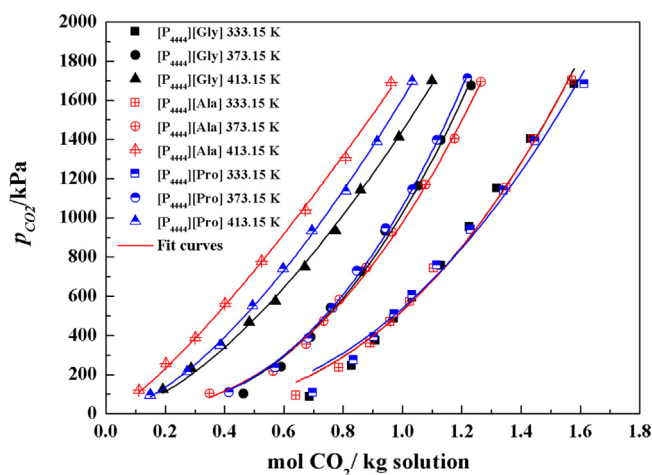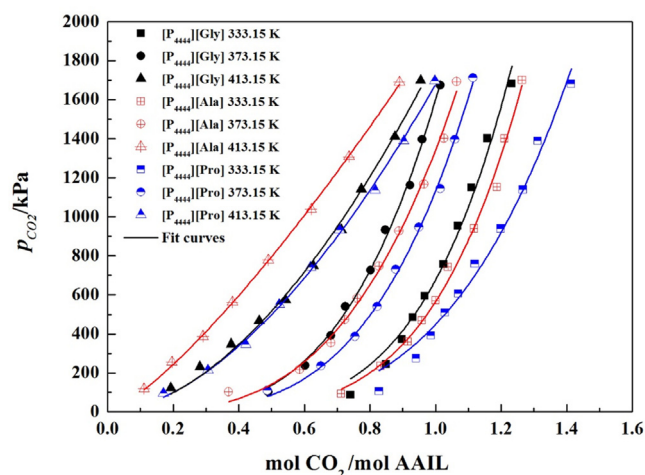
**Fig. 7.** CO$_2$ loading in mixed solvents (30 wt% AAILs + 70 wt% PEG400).

In Fig. 6 it can also be found that the solubility shows a very small difference at 333.15 K and 373.15 K. However, when temperature increases to 414.15 K, the difference in CO$_2$ solubility is noticeable and increases in the following order: [P$_{4444}$][Ala]-PEG400 < [P$_{4444}$][Pro]-PEG400 < [P$_{4444}$][Gly]-PEG400. The relatively low CO$_2$ solubility in [P$_{4444}$][Ala] may be attributed to the steric hindrance around the amino group (caused by the extra methyl group, seen in Fig. 1), resulting in a lower reactivity and CO$_2$ capacity than [P$_{4444}$][Gly].

In order to investigate the influence of chemical structure of the three AAILs on CO$_2$ solubility and the function of the co-solvent PEG, the CO$_2$ sorption capacity is also given as CO$_2$ loading based on $\beta$ (mol CO$_2$/mol AAIL), as shown in Fig. 7. The CO$_2$ loading $\beta$ was calculated by the absorbed CO$_2$ minus the amount of CO$_2$ absorbed by PEG400 according to Henry's law constant (Li et al., 2012a) dividing by the amount of AAILs.

[P$_{4444}$][Pro]-PEG400 shows the best CO$_2$ loading at the investigated temperature and pressure ranges. The CO$_2$ loading of [P$_{4444}$][Pro]-PEG400 reaches around 0.82 mol CO$_2$/mol [P$_{4444}$][Pro] at 333.15 K and 100 kPa, which is higher than that of [P$_{4444}$][Gly]-PEG400 and [P$_{4444}$][Ala]-PEG400 with CO$_2$ loading of around 0.79 mol CO$_2$/mol AAILs. As pressure increases to 1600 kPa, the CO$_2$ loading shows obvious difference. It presents that the CO$_2$ sorption ability of AAILs are ranked as: [P$_{4444}$][Pro] > [P$_{4444}$][Ala] > [P$_{4444}$][Gly]. Some literatures also reported CO$_2$ loading in AAILs (i.e. [P$_{66616}$][Pro] and [P$_{66616}$][Gly]) with [P$_{66616}$]$^+$ as cation at relatively mild conditions (at 295 K and 100 kPa) (Goodrich et al., 2010; Gurkan et al., 2010), but the data at the same conditions is hard to find. In this blend solvent the CO$_2$ loading is significantly higher than 0.5 mol CO$_2$/mol AAILs and approaches 1:1 stoichiometry. It is interesting that the theoretical CO$_2$ capacity in AAIL supported in porous poly(methyl methacrylate) or porous SiO$_2$ is reported to be 1:2 stoichiometry (Wang et al., 2013; Zhang et al., 2006). This suggests that PEG400 as co-solvent may have provided a more efficient gas-liquid interface which enhanced the CO$_2$ sorption in AAILs. The CO$_2$ sorption mechanism of AAILs was reported in literatures (Gurkan et al., 2010; Zhang et al., 2006). To understand the CO$_2$ sorption mechanism with presence of PEG as co-solvent, the FTIR spectra (Thermo Nicolet Nexus 670 FTIR spectrometer) of [P$_{4444}$][Gly]-PEG400 before and after CO$_2$ sorption were investigated, as shown in Fig. 8. The FTIR spectra of [P$_{4444}$][Ala]-PEG400 and [P$_{4444}$][Pro]-PEG400 are shown in Figures SI4 and SI5. The IR spectra of [P$_{4444}$][Gly]-PEG400 contain only one peak at approximately 1589 cm$^{-1}$, corresponding to the CO$_2^-$ group in the AA anion structure. Upon exposure

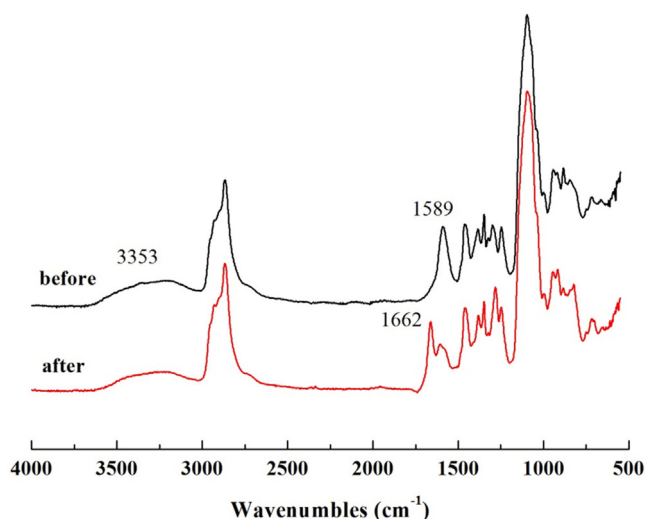**Fig. 6.** CO$_2$ capacity in mixed solvents (30 wt% AAILs + 70 wt% PEG400).

**Fig. 8.** FTIR spectra of $[P_{4444}][Gly]$-PEG400 before and after $CO_2$ sorption.

to $CO_2$ a new peak appeared at approximately 1662 cm$^{-1}$, corresponding to the formation of a new COOH group (Zhang et al., 2006). Moreover, no ammonium formation could be found since there were no ammonium bands between 3000 and 2800 cm$^{-1}$ and combination bands in the 2800–2000 cm$^{-1}$ region (Gurkan et al., 2010; Silverstein et al., 2005). Based on the FTIR analysis and practical $CO_2$ loading, the absorption mechanism of AAILs in PEG400 co-solvent is proposed, as illustrated in Fig. 9. The proposed mechanism of $[P_{4444}][Pro]$-PEG400 absorbing $CO_2$ is the same as that of pure $[P_{66614}][Pro]$ (Gurkan et al., 2010), indicating that PEG400 as a co-solvent is not involved in the reaction. Moreover, these
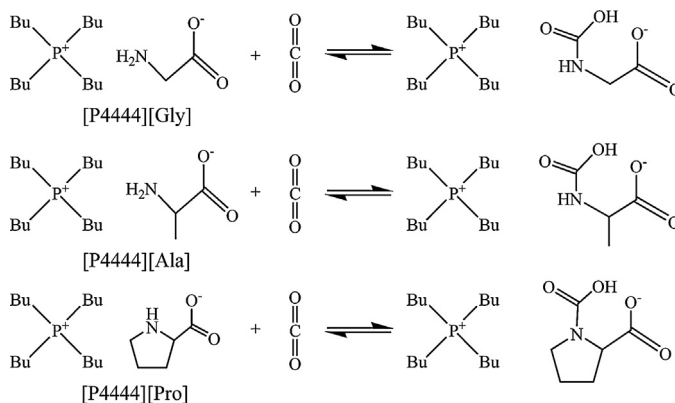


**Fig. 9.** Reaction schematics of $CO_2$ with $[P_{4444}][Gly]$, $[P_{4444}][Ala]$ and $[P_{4444}][Pro]$ with PEG400 as co-solvent.

three typical AAILs studied in this contribution showed the same absorption mechanism.

According to the reaction schematics of $CO_2$ with AAILs, AAILs-carbamates are formed after $CO_2$ sorption, which is confirmed by the formation of very small AAILs-carbamate salt particles during the experiments. These particles are insoluble with PEG400 below 343.15 K, as shown in Fig. 10a. At the beginning of absorption, these particles are well dispersed in PEG400 solution. After standing still for several hours two phases can be observed. These two phases can be easily mixed to form a well-dispersed solvent again simply by shaking the container, as the particles are compatible with PEG400 and their size is very small. SEM (Hitachi S3400 scanning electron microscope) was employed to investigate the particle size, as shown in Fig. 10(b–d), and the particles have a size of about 4 μm, which is much larger than the pore size in the membrane surface layer (~0.01 μm) and much smaller than the pathway in common



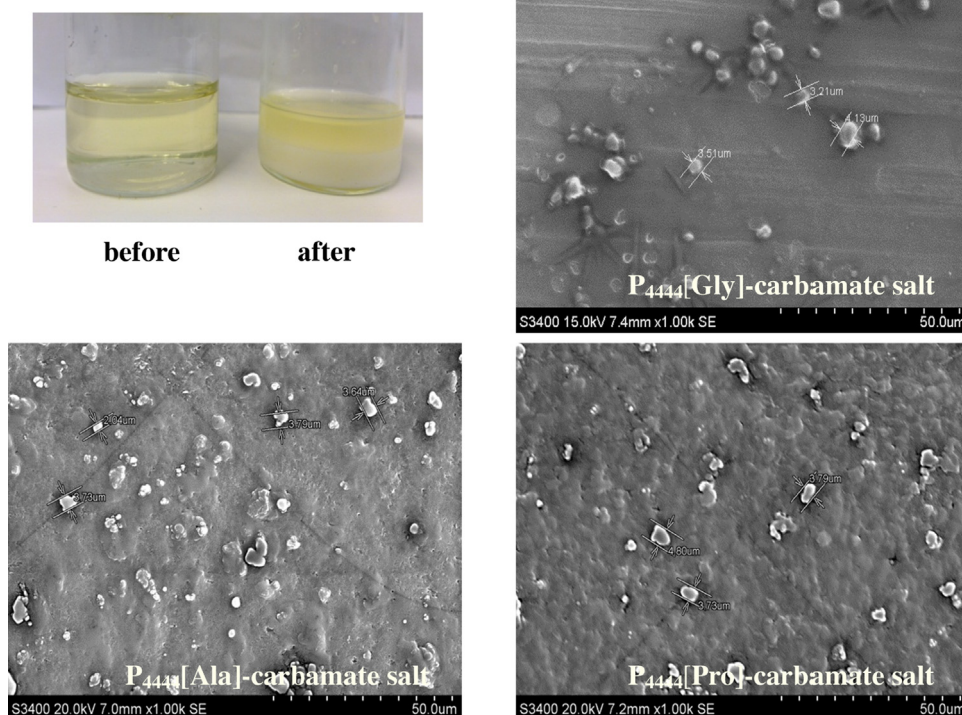**Fig. 10.** Images of AAILs-carbamate salt: (a) AAILs-PEG400 before and after $CO_2$ absorption at 333.15 K; (b) SEM of $[P_{4444}][Gly]$-carbamate salt; (c) SEM of $[P_{4444}][Ala]$-carbamate salt; d SEM of $[P_{4444}][Pro]$-carbamate salt.

hollow fiber membranes (>500 μm) (Mulder, 1996). As a result, the particles can be easily transported as in the two phase flow in the membrane contactor and do not block the pores in membranes.

In general, AAILs become solid after absorbing $CO_2$, which impedes their application in many industrial processes. The application of PEG400 as co-solvent seems able to solve this problem and make more applications possible. It should be noted that particles will be only formed at 333.15 K and 373.15 K for $[P_{4444}][Gly]$ or $[P_{4444}][Ala]$ based mixed solution. When temperature increased to 413.15 K, no particles were found in the solution. In $[P_{4444}][Pro]$ based mixed solution, the particle was formed only at 333.15 K.

The experimental $CO_2$ capacity or loading was used to correlate the $CO_2$ solubility with partial pressure and temperature on the basis of Jou and Mather model (Aziz et al., 2012; Jou and Mather, 2005) and shown in Eqs. (4)–(6):

$$\ln p = A + B \ln \alpha \quad \text{or} \quad \ln p = A + B \ln \beta \tag{4}$$

$$A = a + bT + cT^2 \tag{5}$$

$$B = e + fT + gT^2 \tag{6}$$

where $p$ is the partial pressure of $CO_2$ in kPa, $\alpha$ is the $CO_2$ capacity in the liquid phase in mol $CO_2$/kg solution, $\beta$ is the $CO_2$ loading in mol $CO_2$/mol AAIL, and $T$ is temperature in K. $A$ and $B$ are functions of temperature. The coefficients of correlations are listed in Table 4. Fig. 11 illustrates the comparison between experimental solubility and calculated solubility. It can be found that the experimental results agree very well with the calculated solubility except for a large deviation around solubility of 0.8 with 30% error corresponding to the solubility data at low $CO_2$ partial pressure (<250 kPa) at 313 K (also seen in Figs. 6 and 7). The deviation is believed to be attributed to the particle formation which breaks the vapor liquid

**Table 4**
Coefficients of correlations of $CO_2$ solubility with partial pressure and temperature in mixed solvents AAILs-PEG400.

| Solutions | Coefficients | | | | | |
|---|---|---|---|---|---|---|
| | $a$ | $b$/K$^{-1}$ | $10^4$ $c$/K$^{-2}$ | $d$ | $e$/K$^{-1}$ | $10^4$ $f$/K$^{-2}$ |
| $CO_2$ capacity | | | | | | |
| $[P_{4444}][Gly]$-PEG400 | −26 | 0.1604 | −1.93 | −23.5 | 0.1521 | −2.21 |
| $[P_{4444}][Ala]$-PEG400 | −12.1 | 0.0838 | −0.818 | −24 | 0.1588 | −2.36 |
| $[P_{4444}][Pro]$-PEG400 | −23.6 | 0.1465 | −1.731 | −40.9 | 0.2429 | −3.39 |
| $CO_2$ loading | | | | | | |
| $[P_{4444}][Gly]$-PEG400 | −29.4 | 0.1849 | −2.313 | −13.7 | 0.12738 | −2.18 |
| $[P_{4444}][Ala]$-PEG400 | −19.9 | 0.1296 | −1.530 | −4.7 | 0.08473 | −1.70 |
| $[P_{4444}][Pro]$-PEG400 | −22.4 | 0.1410 | −1.6688 | −60.3 | 0.3707 | −5.34 |
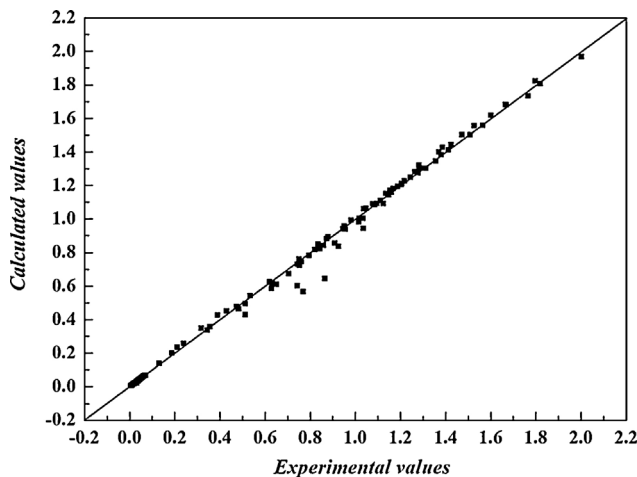


**Fig. 11.** The comparison between experimental $CO_2$ partial pressure and calculated pressure.
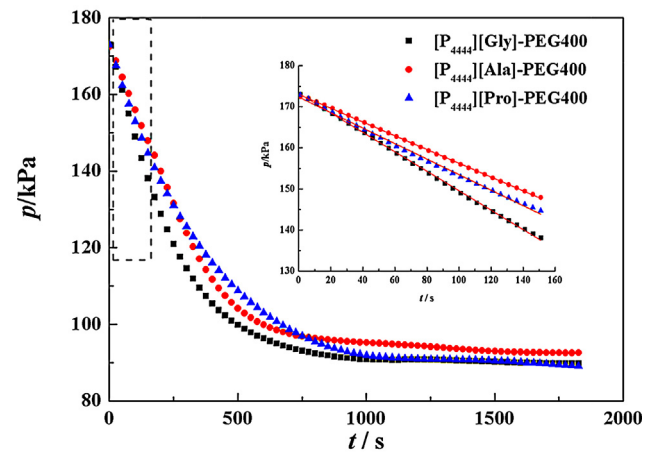


**Fig. 12.** $CO_2$ pressure decay with time in mixed solvent (30 wt% AAILs + 70 wt% PEG400) at 333.15 K.

equilibrium. It can further be proved by the good correlation results at 413 K as no particles are formed at this condition. The total AAD of the model was 3.21%. As a result, the model provides a relatively good correlated result, especially at high temperature and pressure conditions. It should be noted that the model is only a parameterized fit of the data and has no thermodynamic significance, but it can be very useful for the prediction of $CO_2$ solubility at specific conditions in potential industrial applications.

Absorption rate is a very important parameter for evaluating the efficiency of absorbents. Fig. 12 shows the pressure decay with time during the $CO_2$ sorption test at 333.15 K. As it can be seen, the vapor pressures of the three AAILs drop drastically in the first 500 s, then gradually become constant and finally reaches the gas–liquid equilibrium. As the gas phase is merely high purity $CO_2$, the gas side mass transfer resistance is regarded as negligible. At the beginning of the absorption the active sites in the AAILs are abundant, and the absorption rate reaches maximum and remains constant, showing clear slopes that can indicate the absorption rate of the AAILs. In this study the absorption rate ($R_{CO_2}$, mol m$^{-2}$ s$^{-1}$) was calculated by Eq. (7):

$$R_{CO_2} = \frac{dn_{CO_2,L}}{A dt} = -\frac{dn_{CO_2,G}}{A dt} = -\frac{V_G}{ART}\frac{dp_{CO_2}}{dt} \tag{7}$$

where $n_{CO_2,L}$ and $n_{CO_2,G}$ are mole flux of $CO_2$ in liquid phase and gas phase, respectively, $A$ is the gas–liquid interface area in m$^2$ and $V_G$ is the gas phase volume in m$^3$. The $CO_2$ absorption rate of AAILs-PEG400 at 333.15 K and 373.15 K are listed in Table 5. At 333.15 K, the $CO_2$ absorption rates of AAILs–PEG400 blends are ranked as: $[P_{4444}][Gly] > [P_{4444}][Pro] > [P_{4444}][Ala]$. The lowest absorption rate of $[P_{4444}][Ala]$ is probably due to the steric hindrance around the amino group. $[P_{4444}][Pro]$ have the highest viscosity at 333.15 K, which may bring in a higher mass transfer resistance and hence a lower absorption rate. However, when the temperature increased to 373.15 K, the absorption rate of $[P_{4444}][Pro]$ exceeds $[P_{4444}][Gly]$.

**Table 5**
$CO_2$ absorption rate at 333.15 K and 373.15 K $CO_2$ in PEG400 and mixed solvents AAILs-PEG400.

| | $T$/K | $dp/dt$ | $V_g$/cm$^{-3}$ | $R_{CO_2}$/(mol m$^{-2}$ s$^{11}$) |
|---|---|---|---|---|
| $[P_{4444}][Gly]$-PEG400 | 333.15 | −0.237 | 109 | 0.019 |
| $[P_{4444}][Ala]$-PEG400 | 333.15 | −0.168 | 109 | 0.0135 |
| $[P_{4444}][Pro]$-PEG400 | 333.15 | −0.189 | 109 | 0.0155 |
| $[P_{4444}][Gly]$-PEG400 | 373.15 | −0.178 | 109 | 0.0128 |
| $[P_{4444}][Ala]$-PEG400 | 373.15 | −0.123 | 109 | 0.0088 |
| $[P_{4444}][Pro]$-PEG400 | 373.15 | −0.218 | 109 | 0.0156 |
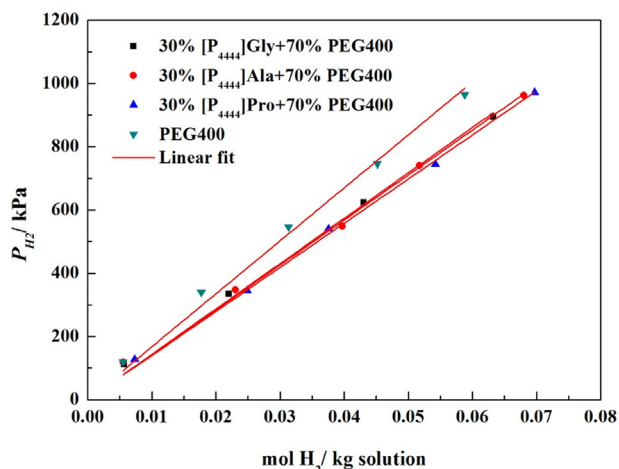
**Fig. 13.** Solubility of $H_2$ in PEG400 and mixed solvents (30 wt% AAILs + 70 wt% PEG400).

**Table 6**
Henry's constant (based on molality) of $H_2$ in PEG400 and mixed solvents AAILs-PEG400 at 333.15 K.

| | $H_b$/(kPa kg mol$^{-1}$) | AAD % |
|---|---|---|
| 30% [P$_{4444}$]Gly + 70% PEG400 | 3586 | 11.47 |
| 30% [P$_{4444}$]Ala + 70% PEG400 | 3553 | 12.1 |
| 30% [P$_{4444}$]Pro + 70% PEG400 | 3489 | 6.04 |
| PEG400 | 4188 | 10.4 |



**Fig. 14.** Ideal $CO_2/H_2$ selectivity at 333.15 K.

This phenomenon may be attributed to the more rapidly decreased viscosity in [P$_{4444}$][Pro] than in [P4444][Gly].

### 3.5. $CO_2/H_2$ selectivity

To capture $CO_2$ from pre-combustion syngas, it is crucial to ensure a high $CO_2/H_2$ selectivity of the developed solvent. The AAILs-PEG400 mixed solvent is a physical solvent toward $H_2$, which leads to an extremely low solubility, especially at high temperatures. Hence, the equilibrium solubility of $H_2$ in mixtures of PEG400 with [P$_{4444}$][Gly], [P$_{4444}$][Ala] and [P$_{4444}$][Pro] was measured only at 333.15 K within a $H_2$ partial pressure range of 100–1000 kPa because the extremely low solubility values at higher temperatures introduces significant errors, and the data are not considered reliable.

Fig. 13 presents the solubility of $H_2$ in PEG400 and AAILs/PEG400 mixed solvents based on $H_2$ loading $\alpha_{H_2}$ (mol $H_2$/kg solution). As shown in the figure, the solubility of $H_2$ in AAILs-PEG400 is much lower than that of $CO_2$ in this mixed solvent. In terms of the overall solubility performance of AAILs-PEG400, there is a very small difference in solubility among these three AAIL-PEG400 absorbents. In addition, it can be found that the solubility of $H_2$ in co-solvent PEG400 is lower than that of the mixed solvents. It is therefore reasonable to assume that AAILs have a higher $H_2$ solubility than PEG400, and the addition of PEG400 as co-solvent increases the $CO_2/H_2$ selectivity.

Since $H_2$ is absorbed by AAILs-PEG400 in physical sorption, Henry's constant based on the molality ($H_b$) was applied to correlate the solubility of $H_2$ in solutions, which is defined as:

$$H_b = \lim_{\alpha_{H_2} \to 0} \frac{f_{H_2}^L(T, P)}{\alpha_{H_2}} \approx \frac{P_e}{\alpha_{H_2}} \qquad (8)$$

where $H_b$ is the Henry's constant based on molality, $\alpha_{H_2}$ is the molality of $H_2$ absorbed in liquid (mol $H_2$/kg total solution), $f_{H_2}^L$ is the fugacity of $H_2$, and $P_e$ is the pressure of system at equilibrium. At a moderate pressure, we assume that $f_{H_2}^L$ equals to $P_e$. The $H_b$ and AAD values of the three AAILs-PEG400 mixed solvents and PEG400 were listed in Table 6. Since the solubility of $H_2$ in solvents is extremely low, a small uncertainty in pressure will result in a large deviation. Hence, the AAD% of $H_2$ solubility is around 10% in this work.

To investigate the $CO_2/H_2$ selectivity at different partial pressure, the ideal selectivity is calculated by Eq. (9):

$$S = \frac{\alpha_{CO_2}}{\alpha_{H_2}} \qquad (9)$$

where $S$ is ideal $CO_2/H_2$ selectivity, $\alpha_{CO_2}$ is $CO_2$ loading calculated by Jou and Mather model, $\alpha_{H_2}$ is $H_2$ loading calculated by $H_b$. As discussed above, there is a larger deviation of $CO_2$ capacity at low partial pressures (e.g. 100 kPa), and thus the experimental data are directly used to calculate $S$ at low partial pressures. For example, $CO_2$ capacity of [P$_{4444}$][Gly]-PEG400 is 0.687 mol $CO_2$/kg solution and the $H_2$ capacity of [P$_{4444}$][Gly]-PEG400 is 0.006 mol $H_2$/kg solution at 333.15 K and 88 kPa. As a result, the ideal $CO_2/H_2$ selectivity is 114.5. The high selectivity means that the solutions can selectively separate $CO_2$ from $H_2$ with very low loss of $H_2$. When partial pressure increases over 200 kPa, $\alpha_{CO_2}$ is calculated by Jou and Mather model. Fig. 14 demonstrates the ideal $CO_2/H_2$ selectivity at different partial pressure. With the increase of partial pressure from around 100 kPa to 2000 kPa, $S$ shows a dramatically decrease from ca 115 to 12. The high selectivity toward $CO_2$ at low pressure was resulted from the high $CO_2$ solubility due to chemisorption. However, when physisorption dominates the absorption process, as discussed above, the solubility gap between $CO_2$ and $H_2$ will be narrowed, which leads to a decreasing of $S$.

### 4. Conclusion

In the present work PEG400 was selected as co-solvent to intensify $CO_2$ sorption in AAILs for pre-combustion $CO_2/H_2$ separation in a membrane contactor. The mixed solution of AAILs and PEG400 shows excellent thermal stability and very low vapor pressure even at 413 K with $N_2$ purging. By introducing PEG400 as co-solvent, the viscosity of mixed solution decreases to be half of that of pure AAILs, which enhances the mass transfer of gases in liquid phase and makes it possible for the application of the AAILs-based solvent in the designed $CO_2$ membrane absorption process. Moreover, PEG400 may have provided a more efficient interface for AAILs to

absorb $CO_2$, approaching the 1:1 stoichiometry. The $CO_2$ sorption mechanism in AAILs-PEG400 is proposed according to the analysis of FTIR results. The $CO_2$ capacity in AAILs-PEG400 reaches 0.687 mol $CO_2$/kg solution at 333 K and 100 kPa, which gives a very high $CO_2$ selectivity over $H_2$ (110).

The selection of the membrane materials and morphology is critical to maintain efficient separation in a membrane contactor. A separate project to study the membranes and membrane/solvent compatibility as well as to evaluate and optimize the membrane absorption system has been on-going in parallel with the current work. The outcome of the membrane related research will be reported elsewhere.

To summarize, the AAILs-PEG400 mixed solvents developed in this work showed high $CO_2$ capacity and $CO_2/H_2$ selectivity, relatively low viscosity, high thermal-stability and very low volatility, which provides an efficient and practical solution for new $CO_2$ capture techniques, especially in membrane contactors and at elevated temperatures. The cost of the AAILs-PEG solvent is mainly from the synthesis of AAILs as PEGs are commercial available at a low cost. Compared to many other task-specific ionic liquids, the relatively simple synthesis by the neutralization reaction of a cation hydroxide solution and amino acid makes the production of AAILs inexpensive and environmentally friendly. These features make AAILs-PEG400 a commercially viable solvent, leading to a great potential for industrial applications.

## Disclosure

The authors declare no competing financial interest.

## Acknowledgements

## Appendix A.  Supplementary data

Supplementary material related to this article can be found, in the online version, at doi:10.1016/j.ijggc.2015.12.027.

## References

Aki, S.N., Mellein, B.R., Saurer, E.M., Brennecke, J.F., 2004. High-pressure phase behavior of carbon dioxide with imidazolium-based ionic liquids. J. Phys. Chem. B 108, 20355–20365.

Aschenbrenner, O., Styring, P., 2010. Comparative study of solvent properties for carbon dioxide absorption. Energy Environ. Sci. 3, 1106.

Aschenbrenner, O., Supasitmongkol, S., Taylor, M., Styring, P., 2009. Measurement of vapour pressures of ionic liquids and other low vapour pressure solvents. Green Chem. 11, 1217–1221.

Aziz, N., Yusoff, R., Aroua, M.K., 2012. Absorption of $CO_2$ in aqueous mixtures of N-methyldiethanolamine and guanidinium tris(pentafluoroethyl)trifluorophosphate ionic liquid at high-pressure. Fluid Phase Equilib. 322-323, 120–125.

Baj, S., Siewniak, A., Chrobok, A., Krawczyk, T., Sobolewski, A., 2012. Monoethanolamine and ionic liquid aqueous solutions as effective systems for $CO_2$ capture. J. Chem. Technol. Biotechnol. 8, 1220–1227.

Bates, E.D., Mayton, R.D., Ntai, I., Davis, J.H., 2002. $CO_2$ captured by a task-specific ionic liquid. J. Am. Chem. Soc. 124, 926–927.

Chakma, A., 1997. $CO_2$ capture processes—opportunities for improved energy efficiencies. Energy Convers. Manage. 38, 51–56.

Chen, J., Spear, S.K., Huddleston, J.G., Rogers, R.D., 2007. Polyethylene glycol and solutions of polyethylene glycol as green reaction media. Green Chem., 64–82.

Dai, Z., Noble, R., Gin, D., Zhang, X., Deng, L., 2016. Combination of ionic liquids with membrane technology: a new approach for $CO_2$ separation. J. Membr. Sci., 1–20.

Davis, R.A., Menbdez, R.E., Sandall, O.C., 1993. Physical, thermodynamic, and transport properties for carbon dioxide and nitrous oxide in solutions of diethanolamine or di-2-propanolamine in polyethylene glycol. J. Chem. Eng. Data 38, 119–124.

Deng, L., Dai, Z., Usman, M., Li, J., 2014. Pre-combustion $CO_2$ Capture Using Membrane Absorption and Ionic Liquids-based Absorbent. ICOM, Suzhou, China.

Fukumoto, K., Yoshizawa, M., Ohno, H., 2005. Room temperature ionic liquids from 20 natural amino acids. J. Am. Chem. Soc. 127, 2398–2399.

Gardas, R.L., Ge, R., Goodrich, P., Hardacre, C., Hussain, A., Rooney, D.W., 2010. Thermophysical properties of amino acid-based ionic liquids. J. Chem. Eng. Data 55, 1505–1515.

Goodrich, B.F., de la Fuente, J.C., Gurkan, B.E., Zadigian, D.J., Price, E.A., Huang, Y., Brennecke, J.F., 2010. Experimental measurements of amine-functionalized anion-tethered ionic liquids with carbon dioxide. Ind. Eng. Chem. Res. 50, 111–118.

Gurkan, B.E., de la Fuente, J.C., Mindrup, E.M., Ficke, L.E., Goodrich, B.F., Price, E.A., Schneider, W.F., Brennecke, J.F., 2010. Equimolar $CO_2$ absorption by anion-functionalized ionic liquids. J. Am. Chem. Soc. 132, 2116–2117.

Hägg, M.-B., Deng, L., 2015. Membranes in gas separation. In: Handbook of Handbook of Membrane Separations: Chemical, Pharmaceutical, Food, and Biotechnological Applications, 2nd ed. CRC Press (Chapter 7).

Hasib-ur-Rahman, M., Siaj, M., Larachi, F., 2012. $CO_2$ capture in alkanolamine/room-temperature ionic liquid emulsions: a viable approach with carbamate crystallization and curbed corrosion behavior. Int. J. Greenh. Gas Control 6, 246–252.

Hasib, M., Bouteldja, H., Fongarland, P., Siaj, M., Larachi, F., 2012. Corrosion behavior of carbon steel in alkanolamine/room-temperature ionic liquid based $CO_2$ capture systems. Ind. Eng. Chem. Res. 51, 8711–8718.

Jing, G., Zhou, L., Zhou, Z., 2012. Characterization and kinetics of carbon dioxide absorption into aqueous tetramethylammonium glycinate solution. Chem. Eng. J. 181–182, 85–92.

Jou, F.Y., Mather, A.E., 2005. Solubility of carbon dioxide in an aqueous mixture of methyldiethanolamine and N-methylpyrrolidone at elevated pressures. Fluid Phase Equilib. 228–229, 465–469.

Kagimoto, J., Fukumoto, K., Ohno, H., 2006. Effect of tetrabutylphosphonium cation on the physico-chemical properties of amino-acid ionic liquids. Chem. Commun. 21, 2254–2256.

Lee, A.S., Eslick, J.C., Miller, D.C., Kitchin, J.R., 2013. Comparisons of amine solvents for post-combustion $CO_2$ capture: a multi-objective analysis approach. Int. J. Greenh. Gas Control 18, 68–74.

Li, J., Chen, L., Ye, Y., Qi, Z., 2014. Solubility of $CO_2$ in the mixed solvent system of alkanolamines and poly(ethylene glycol) 200. J. Chem. Eng. Data 59, 1781–1787.

Li, J., Ye, Y., Chen, L., Qi, Z., 2012a. Solubilities of $CO_2$ in poly(ethylene glycols) from (303.15 to 333.15) K. J. Chem. Eng. Data 57, 610–612.

Li, J., You, C., Chen, L., Ye, Y., Qi, Z., Sundmacher, K., 2012b. Dynamics of $CO_2$ absorption and desorption processes in alkanolamine with co-solvent polyethylene glycol. Ind. Eng. Chem. Res. 51, 12081–12088.

Li, X., Hou, M., Zhang, Z., Han, B., Yang, G., Wang, X., Zou, L., 2008. Absorption of $CO_2$ by ionic liquid/polyethylene glycol mixture and the thermodynamic parameters. Green Chem. 10, 879–884.

Mulder, M., 1996. Basic Principles of Membrane Technology Second Edition. Kluwer Academic Pub.

Notz, R., Tonnies, I., McCann, N., Scheffknecht, G., Hasse, H., 2011. $CO_2$ capture for fossil fuel-fired power plants. Chem. Eng. Technol. 34, 163–172.

Ohno, H., Fukumoto, K., 2007. Amino acid ionic liquids. Acc. Chem. Res. 40, 1122–1129.

Shannon, M.S., Bara, J.E., 2011. Properties of alkylimidazoles as solvents for $CO_2$ capture and comparisons to imidazolium-based ionic liquids. Ind. Eng. Chem. Res. 50, 8665–8677.

Silverstein, R.M., Webster, F.X., Kiemle, D.J., 2005. Spectrometric Identification of Organic Compounds, 7th ed. John Wiley & Sons, Inc., New York.

Simons, K., Nijmeijer, K., Wessling, M., 2009. Gas–liquid membrane contactors for $CO_2$ removal. J. Membr. Sci. 340, 214–220.

Zhang, S.J., Zhang, X., Zhao, Y., Zhao, G., Yao, X., Yao, H., 2010. A novel ionic liquids-based scrubbing process for efficient $CO_2$ capture. Sci. China Chem. 53, 1549–1553.

Trivedi, S., Pandey, S., 2011. Interactions within a ionic liquid plus poly(ethylene glycol) mixture revealed by temperature-dependent synergistic dynamic viscosity and probe-reported microviscosity. J. Phys. Chem. B 115, 7405–7416.

Wang, X., Akhmedov, N.G., Duan, Y., Luebke, D., Hopkinson, D., Li, B., 2013. Amino acid-functionalized ionic liquid solid sorbents for post-combustion carbon capture. ACS Appl. Mater. Interfaces 5, 8670–8677.

Yang, Z.-Z., He, L.-N., Zhao, Y.-N., Li, B., Yu, B., 2011. $CO_2$ capture and activation by superbase/polyethylene glycol and its subsequent conversion. Energy Environ. Sci. 4, 3971–3975.

Zhang, J., Zhang, S., Dong, K., Zhang, Y., Shen, Y., Lv, X., 2006. Supported absorption of $CO_2$ by tetrabutylphosphonium amino acid ionic liquids. Chem.-Eur. J. 12, 4021–4026.

Zhang, X.P., Zhang, X.C., Dong, H.F., Zhao, Z.J., Zhang, S.J., Huang, Y., 2012. Carbon capture with ionic liquids: overview and progress. Energy Environ. Sci. 5, 6668–6681.